

Processing and Properties of Cluster Strengthened Aluminium Alloys

S.P Ringer¹

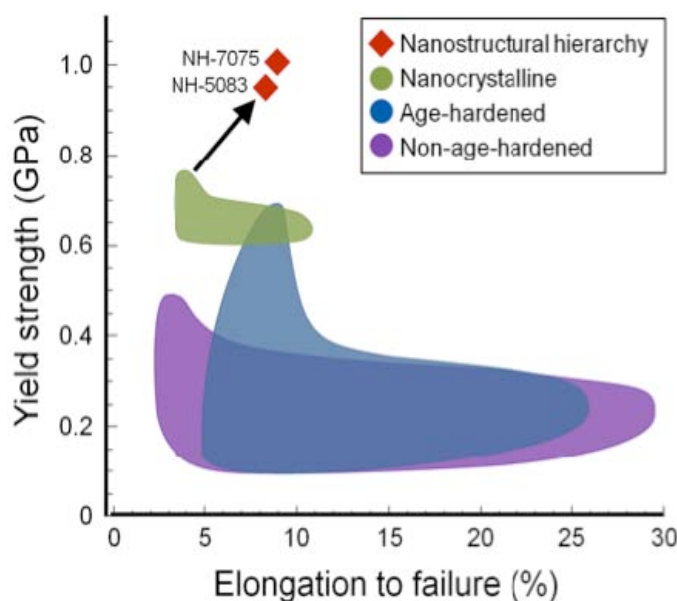
¹Australian Centre for Microscopy & Microanalysis, The University of Sydney, NSW, 2006, Australia

This paper summarises recent research on the processing and properties of Al alloys that exhibit cluster strengthening, as a result of a highly inhomogeneous or clustered state of solute in the supersaturated solid solution. We show that the fraction of solute tied to clusters changes dramatically during the early stages of conventional ageing of an Al-Zn-Mg-Cu alloy. Severe plastic deformation is also demonstrated as an alternative means of creating a clustered solute arrangement in a commercial 7075 alloy that exhibits a remarkable yield strength of ~ 1 GPa with reasonable ductility. We discuss lattice rectification in atom probe microscopy and the way that this is guiding computational research on the energy landscape of a dislocation moving through a dispersion of solute clusters.

Keywords: Cluster strengthening, precipitation strengthening, atom probe microscopy, molecular dynamics.

1. Introduction

Atomic clustering of solute elements during phase decomposition in multi-component alloys is a topic of increasing interest in materials science and engineering because of the potential for clusters to change materials properties and/or for the clusters to control phase transformation pathways. The ICAA series of conferences have successfully tracked progress of these developments in the context of Al alloys, with particular focus on the microstructure and properties of wrought alloys. This is a burgeoning field of research where there remain many important questions of both fundamental and technological significance. Descriptions of how clustering might influence strength, work hardening and transformation pathways require a phenomenological and mechanistic framework derived from experimental insights into the temporal evolution of actual atomistic processes during decomposition and deformation. Ideally, this information would be based on direct microscopic imaging, though such experiments are very challenging and so we remain at a tantalising frontier of understanding the nexus between clustering, precipitation, alloy processing and strengthening. This said, there has been significant recent progress and new insights are emerging as a result of developments in atom probe microscopy. Significantly, the capacity for direct microscopic imaging



coupled with the excellent counting statistics available in atom probe means that the data is well matched to guide atomistic modeling and simulation. This paper summarises recent research using these techniques to explore the role of Cu in Al alloys processed conventionally and by high-pressure torsion (HPT).

Figure 1. Yield strength-elongation to failure for various classes of Al alloys. The 7075 and 5083 tensile data is by M.Y. Murashkin and R. Valiev.

2. Clustering and Strengthening in Al-Zn-Mg-Cu (7xxx) Alloys

2.1 Conventional Thermomechanical Processing

Figure 1 is a chart of the yield strength versus elongation for a wide range of metallic Al alloys. The familiar conflict between these two properties is seen and a survey of property-performance space indicates that values of yield strength ~ 0.7 GPa represents the current strength record for precipitation-strengthened wrought Al alloys. The specific data for commercial 7075 is included as an example of a high strength alloy. Figure 2(a) shows the age hardening response from an experimental Al-2Zn-1.9Mg (at. %) alloy with, and without, an addition of 0.7 at. % Cu. As previously reported, this composition gives rise to a remarkable rapid hardening effect [1]. We have undertaken careful atom probe experiments of the base ternary and Cu-bearing quaternary alloys and results are provided in Fig. 2(b) for the as-quenched (AQ) condition, after quenching from a solution treatment at 525 °C, and after ageing at 150 °C for 30 sec and 60 sec. Only Mg, Zn and Cu solute atoms are rendered in these tomograms and the particular solutes are not distinguished. The details of the atom probe techniques used to generate these images and data are provided elsewhere [1].

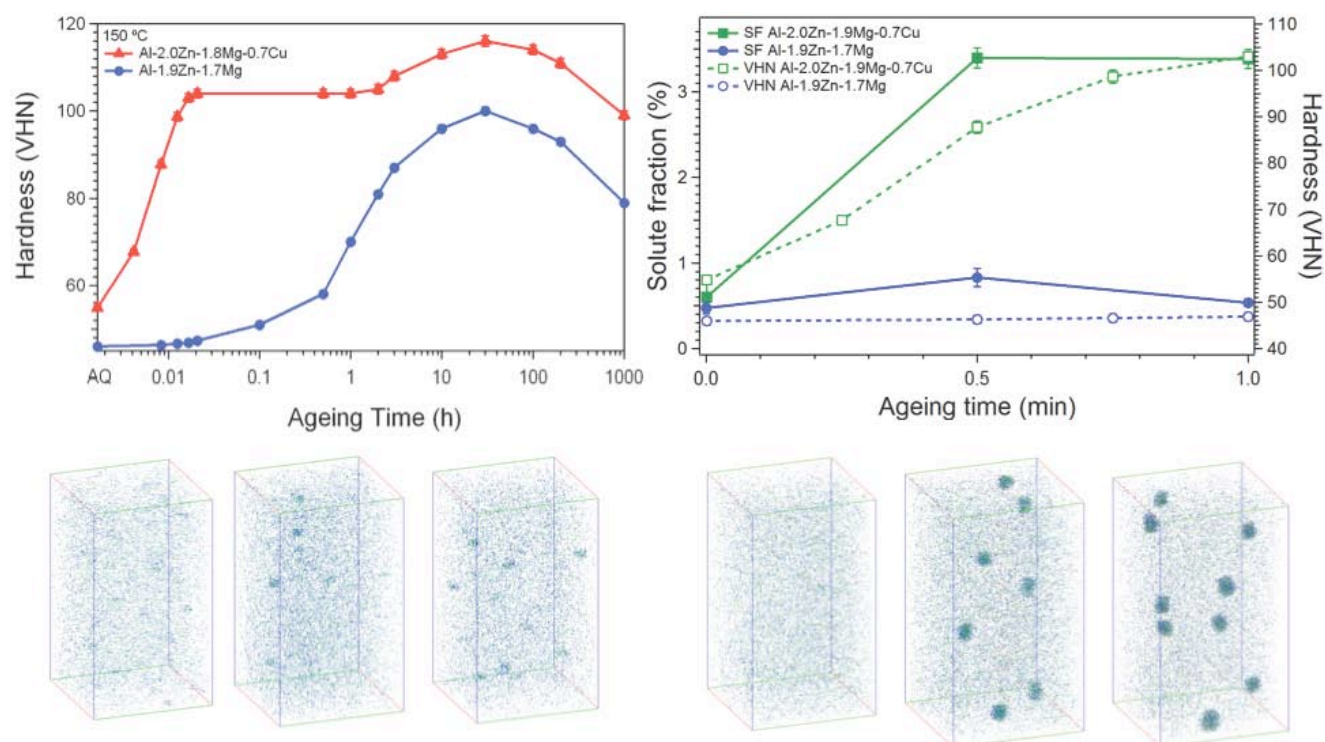


Figure 2. (a) Age hardening response of Al-2Zn-1.9Mg-(0.7Cu) at. %. (b) Atom maps of Zn, Mg and Cu solute (i-iii) for the ternary and (iv-vi) for the quaternary alloy. (c) Correlation of solute fraction tied to clusters and hardness as a function of ageing time. (Data by P.V. Liddicoat).

In the AQ condition, the solute appear at a coarse level of inspection to be uniform, though more careful analyses have demonstrated that there is, in fact, significant atomic clustering within these solute atom distributions and that the solute is far from randomly arranged. Undoubtedly, this seeds much of the subsequent microstructural evolution in the alloy. We refer to this as atomic clustering, because the effects are so very fine and involve a small number (< 10) atoms. After ageing for 30 sec at 150 °C, we see that the ternary alloy exhibits distinct evidence of larger clusters, several nanometers in dimension. These nanoscale or nano-clusters contain > 20 atoms and are dispersed very finely, having a number density of $\sim 10^{17} \text{ cm}^{-3}$. The occurrence of these nano-clusters contributes a hierarchical structure to the alloy, since the solute atoms between them are also clustered in the same general way that they were in the AQ condition. The hierarchy of solute

structures thus involves high number density of nano-clusters, having a number density of $\sim 10^{17} \text{ cm}^{-3}$, together with a very fine dispersion of atomic clusters having a number density of $\sim 10^{18} \text{ cm}^{-3}$. It may be noted that TEM of these alloys is very challenging and that our previous experiments have provided no evidence of second phase precipitation in the ternary alloy until ageing at $150 \text{ }^\circ\text{C}$ had proceeded to $\sim 2.5 \text{ h}$. The observations in the Cu-bearing quaternary alloy are similar: we observe atomic clustering of the Mg, Zn and Cu solute atoms in all conditions, including the AQ condition and detect nano-clusters of these species after ageing at $150 \text{ }^\circ\text{C}$ for 30 sec. These are larger and more numerous after ageing for 60 sec. Closer analysis reveals a striking contrast between the results for the two alloys: firstly, the presence of Cu has triggered a catalytic clustering reaction and there is a higher number density by a factor 2-3 both of the atomic clusters and the nano-clusters. The nano-clusters present Cu-bearing alloy are larger and more numerous than those in the ternary alloy. Though many aspects of these clusters could be compared and contrasted, we focus here on the fraction of total solute that is bound up or structured, either in atomic clusters or nano-clusters. The results are provided in Fig. 2(c), which also includes the hardness traces for the respective conditions of each alloy. The catalytic action of the Cu is clearly demonstrated insofar as both alloys have a similar fraction of $\sim 0.5\%$ of the alloy total solute content that is bound to clusters in the AQ condition. However, after just 30 sec at $150 \text{ }^\circ\text{C}$, this fraction is $\sim 7 \times$ higher at 3.5% in the Cu-bearing quaternary alloy whereas it is barely unchanged in the ternary alloy. Consider that this alloy contains a total of $4.7 \text{ at. } \%$ solute and that this extent of clustering implies that the alloy has $\sim 0.16 \text{ at. } \%$ of all solute clustered after just 60 sec of ageing. The correlation with the hardening trends is also striking.

2.2 Processing Using Severe Plastic Deformation

Figure 1 suggests that a revolutionary new design of alloy microstructure is required to break the notional strength record whilst, ideally, retaining ductility. Figure 2 indicates that atomic clustering can contribute significantly to strengthening in conventionally processed alloys. These alloys are subjected to a solution treatment, followed by a water quench and elevated temperature ageing. These thermal treatments exploit the alloy phase equilibria to set up driving forces for particular arrangements of solute atoms, including a large driving force for the precipitation of second phases. Recently, we have sought to use severe plastic deformation as an alternate approach to drive rearrangements of solute. Starting from the quenched-in nanostructure of the AQ condition, we have applied high-pressure torsion to 7075 and 5083 (Al-Mg-Sc alloy). The resulting mechanical properties are truly remarkable and are charted in Fig. 1. They are seen to break the notional strength ceiling for a metallic Al alloy and maintain reasonable levels of ductility.

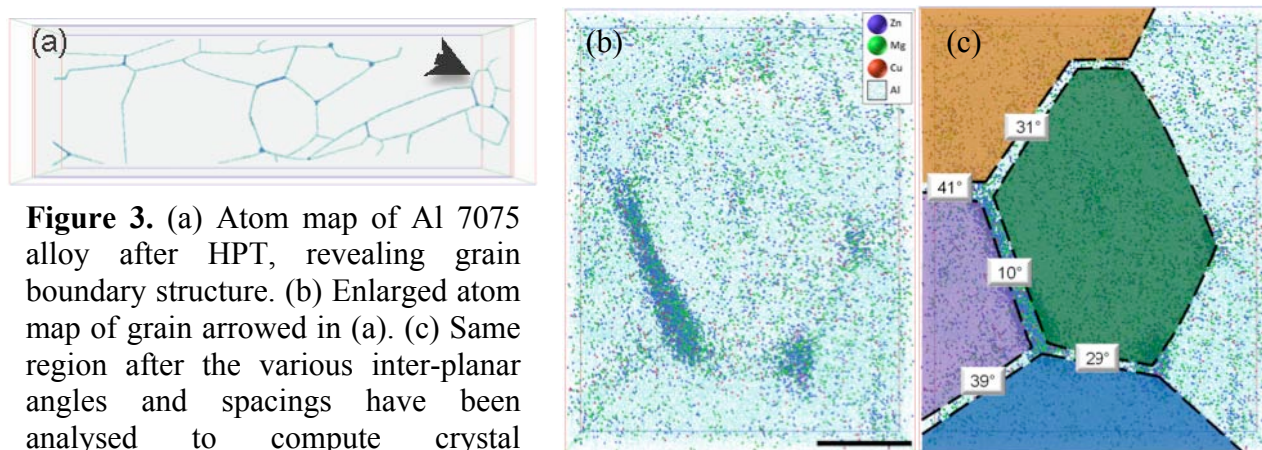


Figure 3. (a) Atom map of Al 7075 alloy after HPT, revealing grain boundary structure. (b) Enlarged atom map of grain arrowed in (a). (c) Same region after the various inter-planar angles and spacings have been analysed to compute crystal misorientations. Data in (a) is $500 \mu\text{m}$ wide. Scale bar in (b) is 5 nm . (Data by P.V. Liddicoat).

Figure 3(a) is a thin ~ 2 nm slice through a very large atom probe data set ~ 0.5 μm wide recorded from the 7075 alloy after the HPT treatment. The atom map has been filtered so as to reveal only the grain boundary regions and demonstrates the extremely fine grain size which was, on average ~ 26 nm in diameter. Inspection reveals that the grain boundaries are structured by solute atoms: nodal aggregates of solute occur at grain boundary junctions and lineal aggregates of solute were observed along certain grain boundaries. A small grain towards the right-hand side of the data slice in Fig. 3(a) is enlarged in Figs. 3(b-c). The atom map of Fig. 3(b) reveals the Zn, Mg and Cu solute atoms and demonstrates that there are fine-scale intragranular atomic clusters and the aforementioned intergranular solute structures. This remarkable microstructure is the result of the severe plastic deformation sweeping solute into a new hierarchical architecture that, together with the grain structure itself, provides record levels of strength. The tendency for the lineal structures to occur on grain boundaries was tested as a function of grain boundary misorientation. The grain misorientation were computed using the same approach as is done in electron backscattered diffraction after planes were identified in each crystal and are indicated in Fig. 3(c). Interestingly, the lineal solute structures tended to occur at the lower angle grain boundaries.

3. A Closer Look at Atomic Clustering

The atom probe experiments described above and others like them provide a highly detailed analysis of the solute distributions in multi-component systems. We recently demonstrated that the resolution of atom probe microscopy is well below 50 pico-metres (pm) in the z-direction and ~ 100 -150 pm in the x-y planes [2]. The fact that the atom maps detail the crystal lattice planes has led us to develop a lattice rectification procedure that allows each individual atom position recorded on the atom probe detector to be shuffled in a systematic and rigorous way to a lattice site. The result of this procedure is demonstrated in Fig. 4 for an Al-2.5Cu-1.5Mg (wt. %) alloy after brief heat treatment at 150 $^{\circ}\text{C}$ to invoke a rapid hardening reaction [3].

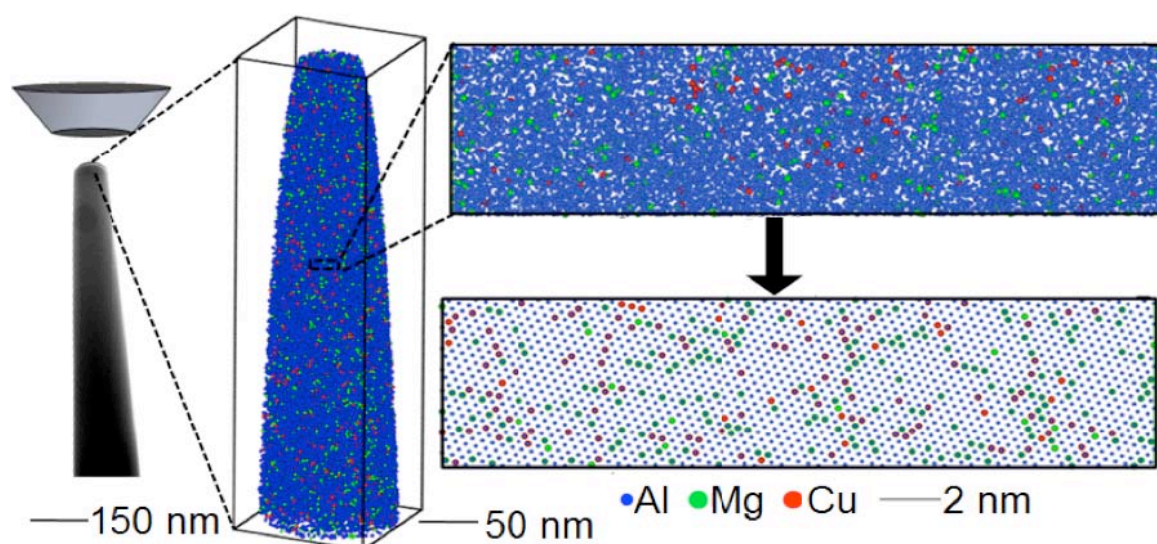


Figure 4. Lattice rectification in atom probe microscopy. True atomic positions are rectified from the raw data. (Data by Dr. R.K.W. Marceau and analysis by Dr. M.P. Moody).

The various length scales are highlighted here: the left-hand side image is a transmission electron microscope (TEM) image of an atom probe specimen, which is in the form a sharp needle-like tip ahead of an extraction electrode that is used to ionize and so finesse the atoms away from the specimen surface towards a time-of-flight detector. Actual (raw) atom probe data is provided in the middle figure reconstructed from the very apex of the specimen tip, which is ~ 50 nm in width. A small region from within this atom probe data is subsequently enlarged at the right-hand side. The

upper right figure is the raw data and the lower right side reveals the atom positions following the lattice rectification procedure. The 3D architecture of the solute arrangements are now imaged directly and are available for species-specific quantitative analysis at a level of detail that is, to our knowledge, beyond that previously available via any other technique. We expect that this technique will influence significantly the characterisation and design of light alloys.

4. Computational Approach to Cluster Hardening

Figure 4 suggests that advances in microscopy have enabled great progress in the quest to achieve direct imaging individual solute atoms and clusters consisting of just a few solute atoms. Indeed, the experimental 3D solute architecture available in these tomographic images sets critical boundary conditions that enable modeling and computational approaches for exploring the transformation pathways and the response to (e.g.) applied deformation. Computational approaches at the appropriate length and time scales are necessary to provide insights into the role of solute atoms and small solute clusters on dislocation motion at the atomic scale. Indeed, that significant strengthening has been demonstrated in materials where there clearly were no second-phase precipitates, highlights an acute need to revisit the physical basis for strengthening in these more complex solid solutions. Classical linear elastic theories of solid-solution strengthening treat the dislocation–solute-atom interaction as having a par elastic component proportional to r^{-1} and a dielastic component proportional to r^{-2} , where r is the distance between the dislocation core and the obstacle. These treatments break down when the dislocation core is in contact with obstacles such as solute atom clusters, where r approaches zero, because atomic mechanisms dominate and the fundamental atomic architecture of the obstacle becomes a key input into the interaction. The complexities require computational approaches and we have used molecular dynamics (MD) approaches. The potential for complexity in this problem is very high and so before computing the deformation of multicomponent volumes such as in Fig. 4, we have tackled binary Al-Cu using an embedded atom method, using potentials due to Liu [4]. A periodic simulation cell geometry containing three blocks of material was used whereby the middle block included an edge dislocation in a glide plane at the centre of the cell. During MD simulations, atoms in upper and lower blocks were frozen, whilst atoms in the central block were mobile. To impose shear on the cell, the upper block was displaced rigidly in the x-direction, whilst the lower block was held fixed.

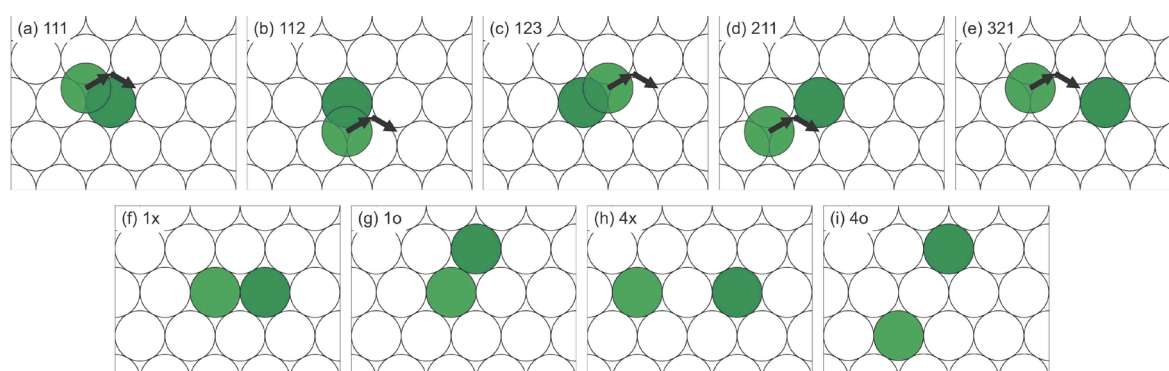


Figure 5. Simulation geometry for an arrangement of two Cu atoms in a di-mer. The illustrations show a projection onto the x-z plane. In (a)-(e), the two Cu atoms cross the glide plane. The arrows indicate how the di-mer arrangement is altered by the passage of an edge dislocation dissociated into two partial dislocations. The designation for these pairs indicates the nearest-neighbor relationship between the atoms at each stage. In pair arrangements (f)-(i), the two Cu atoms are on the same side of the glide plane. The designation for these pairs indicates the nearest neighbor relationship of the atoms (1 or 4), and whether the pair is aligned with the x-axis or not (x or o). There are corresponding arrangements above and below the glide plane. (Figure by Dr. R. Powles).

Figure 5 describes our simulation geometry and notation for a pair of Cu atoms (di-mer) that either cross, or are on the same side as the glide plane. Figure 6(a-b) is a selection of our recent computational results and charts the interaction energies between a Cu di-mer and an edge dislocation. The interaction energies of the crossing di-mer configurations, Fig. 6(a), are all negative, indicating that these solute arrangements attract the dislocation. For the non-crossing di-mer configurations, Fig. 6(b), the interactions are attractive for di-mers above the glide plane and generally negative and smaller in magnitude for di-mers below the glide plane. Interestingly, the interaction energies of the non-crossing di-mers situated above the glide plane are larger in magnitude than those of the crossing pairs. Since the pairs are not rearranged by the passage of the dislocation, no net energy change is observed. These results point to the significant amount of computational modelling required to better understand the role of solute architecture on the strength and work hardening characteristics of Al alloys.

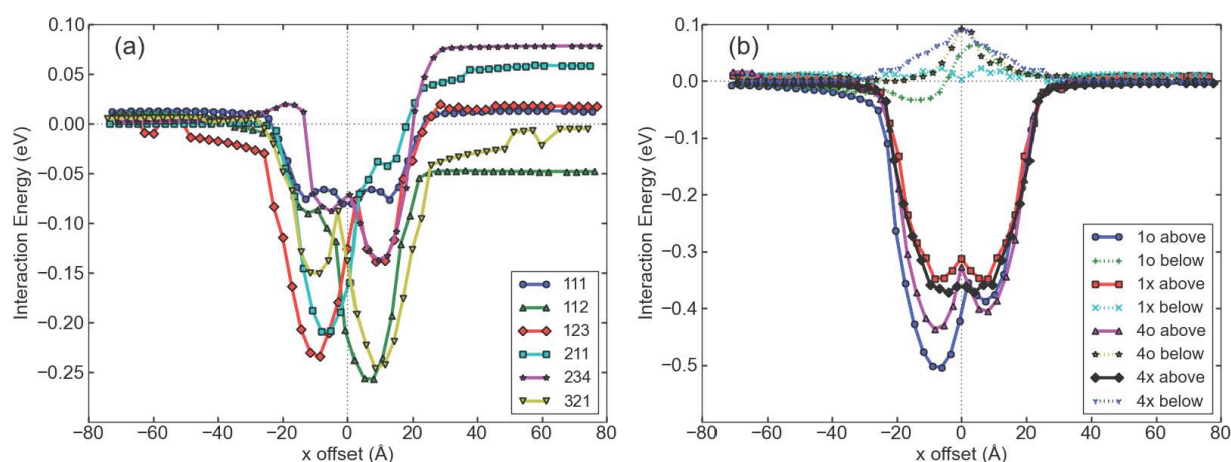


Figure 6. Interaction energies between an edge dislocation Cu atom di-mers in the configurations described in Fig. 2. Results are for di-mers that (a) cross and (b) are on the same side (above or below) of the glide plane. Di-mers that cross the glide plane are rearranged by the passage of the dislocation, which can lead to a net change in the configurational energy. Di-mer configurations are identified using the same notation as in Fig 5. (Figure by Dr. R. Powles).

5. Summary

The *fraction* of clustered solute is an important parameter in understanding the effects of clustering and hardening. Severe plastic deformation can be used to create entirely new hierarchical solute architectures with remarkable combinations of mechanical properties. As microscopy brings us closer to an ultimate whereby 3D atomic positions for all species are available, the connections between computational and experimental approaches will grow. The interaction of Cu di-mers on the same side of the glide plane was demonstrated as higher than those crossing the glide plane.

Acknowledgements

The author is grateful for stimulating collaboration with all past and present students and research associates. In particular, Drs. Liddicoat, Marceau, Moody, Powles and Stephenson from the University of Sydney are thanked. Mechanical property data in Fig. 1 are courtesy of Prof. R. Valiev, Ufa University, Russia. The scientific support of staff at the AMMRF and funding from the Australian Research Council and University of Sydney are gratefully acknowledged.

References

- [1] P.V. Liddicoat and S.P. Ringer: elsewhere in Proceedings of the 12th International Conference on Aluminium Alloys.
- [2] B. Gault, M.P. Moody, F. de Geuser, D. Haley, L.T. Stephenson and S.P. Ringer: *Appl. Phys. Letts.* 95 (2009) 034103.
- [3] R.K.W. Marceau, G. Sha, R. Ferragut, A. Dupasquier and S.P. Ringer: *Acta Mater.* (2010) In press, doi:10.1016/j.actamat.2010.05.020.
- [4] X. Liu, NIST Interatomic Potentials Repository: <http://www.ctcms.nist.gov/potentials>.